Droop Control with an Adjustable Complex Virtual Impedance Loop based on Cloud Model Theory

Li, Yan; Shuai, Zhikang; Xu, Qinming; Guerrero, Josep M.

Published in:
Proceedings of IECON 2016: 42nd Annual Conference of the IEEE Industrial Electronics Society

DOI (link to publication from Publisher):
10.1109/IECON.2016.7793521

Publication date:
2016

Document Version
Early version, also known as pre-print

Citation for published version (APA):
Li, Y., Shuai, Z., Xu, Q., & Guerrero, J. M. (2016). Droop Control with an Adjustable Complex Virtual Impedance Loop based on Cloud Model Theory. In *Proceedings of IECON 2016: 42nd Annual Conference of the IEEE Industrial Electronics Society* (pp. 3223 - 3228). IEEE Press. https://doi.org/10.1109/IECON.2016.7793521

Droop Control with an Adjustable Complex Virtual Impedance Loop based on Cloud Model Theory

Yan Li
School of information science and engineering
Central South University
Changsha, China
liyanly76@gmail.com

Zhikang Shuai, Qinming Xu
College of Electrical and Information Engineering
Hunan University
Changsha, China
Josep M. Guerrero, *Fellow, IEEE*
Department of Energy Technology
Aalborg University,
Aalborg, Denmark
joz@et.aau.dk

***Abstract*—Droop control framework with an adjustable virtual impedance loop is proposed in this paper, which is based on the cloud model theory. The proposed virtual impedance loop includes two terms: a negative virtual resistor and an adjustable virtual inductance. The negative virtual resistor term not only can avoid the active/reactive power coupling, but also it may reduce the output voltage drop of the PCC voltage. The proposed adjustable complex virtual impedance loop is putted into the conventional P/Q droop control to overcome the difficulty of getting the line impedance, which may change sometimes. The cloud model theory is applied to get online the changing line impedance value, which relies on the relevance of the reactive power responding the changing line impedance. The verification of the proposed control strategy is done according to the simulation in a low voltage microgrid in Matlab.**

***Keywords*—microgrid, droop control, adjustable virtual impedance, membership cloud**

I. INTRODUCTION

In order to manage the widespread penetration of renewable energy and distributed generation (DG) in power distribution networks, the microgrid concept was introduced into electric power systems. The microgrid approach offers the most flexibility and reliability for power systems, and thus the micro-grid is generally regarded as the most attractive DG system configuration [1]-[2].

The active power-frequency droop (*P-f* droop) and the reactive power-voltage droop (*P-V* droop) is used to realize the "*plug and play*" characteristic (*PnP*) and to mimic the parallel operation characteristics of synchronous generators, which was initially proposed in [1] for the parallel operation of multiple uninterruptible power supply units [3].There are mostly the resistive lines in low voltage microgrids [4]. The high resistive value of distribution lines makes the control method of active power (*P*) and reactive power (*Q*) couple. The accuracy of *Q*-control in grid-connected operation mode and the *Q*-sharing during in islanding mode are affected due to the unequal voltage drops along the microgrid with the impaired line impedances and the inverter output impedances significantly [5]. Note that voltage is a local variable in the microgrid, while frequency is a global one.

A lot of research works have been done to diminish the abovementioned disadvantages of the traditional droop control. We found out mainly three kinds of methods to perform this:

(i) To make the inverter output impedance to be inductive instead of resistive, controlling parameters can be setting. However, it is important for this method to rely on the power stage and the control parameters of the voltage and current loops, which may trade-off the system stability.

(ii) To solve this problem, Guerrero [7] proposed the control strategy based on the virtual impedance. In order to ensure the inverter output impedance adjusted flexibly, it is necessary to feed back the inverter output current in the virtual impedance loop. It seems to be a good way to diminish problem of power coupling and guarantee *Q*-sharing by the virtual impedance [8]. But the control strategy based on the virtual impedance may cause DG voltage distortions because of bad designed or implemented. Therefore the system stability and dynamics are adversely affected [9].

(iii) A droop control method connecting an adjustable virtual impedance is proposed to decrease mismatch voltage drops across lines and to diminish *P/Q* coupling in this paper. The adjustable virtual impedance is regulated the cloud model theory.

This paper starts in Section II, which discusses firstly some problems about *P/Q* coupling and mismatch line impedances among inverters in a microgrid. Section III shows the proposed droop controlling method with the cloud-based adjustable virtual impedance. The simulation is done in Section IV. The system performance is verified by the simulating results. Section V is the conclusions.

II. PROBLEMS ON POWER COUPLING AND IMBALANCE LINE IMPEDANCES

The voltage across the equivalent line impedance is shown in Fig.1. Note that the inverter output impedance is included the equivalent line impedance.

This work is supported by National Nature Science Foundation under Grant 51507192, China .

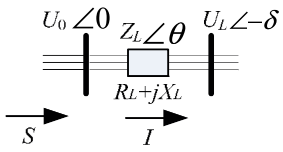

Fig. 1. the line impedance voltage.

From the Fig.1 we can see that the voltage drop (ΔU_L), and the phase angle (δ) difference can be calculated as follows

$$\Delta U_L = U_0 - U_L \approx \frac{R_L P + X_L Q}{U_0} \tag{1}$$

$$\delta = \frac{X_L P - R_L Q}{U_0} \tag{2}$$

Where $U_0\angle 0$ denotes the inverter open-circuit voltage and $U_L\angle\text{-}\delta$ the voltage on PCC, respectively; and $Z_L\angle\theta = R_L + jX_L$ is the line impedance of the system. From (1) and (2), it can be seen that the higher the R_L/X_L ratio of the distribution feeders, the higher the *P/Q* coupling. Actually, besides the *P/Q* coupling effect, the power sharing among the inverters is affected by the mismatch line impedance. For instance, consider that the two DGs present same line impedances R_L+jX_L is not realistic. The line impedances may change due to many factors. The changing line impedances can be given as in the resistive and/or inductive parts, ΔR and ΔX respectively. Consequently this imbalance may produce voltage differences ΔU and circulating currents, thus these imbalance line impedances ΔR and ΔX may bring about unequal *Q*-sharing. For this case, the total line impedance is presented as:

$$\vec{Z}_T = R_L + \Delta R + j\omega(X_L + \Delta X) \tag{3}$$

Notice that it includes nominal values and variations.

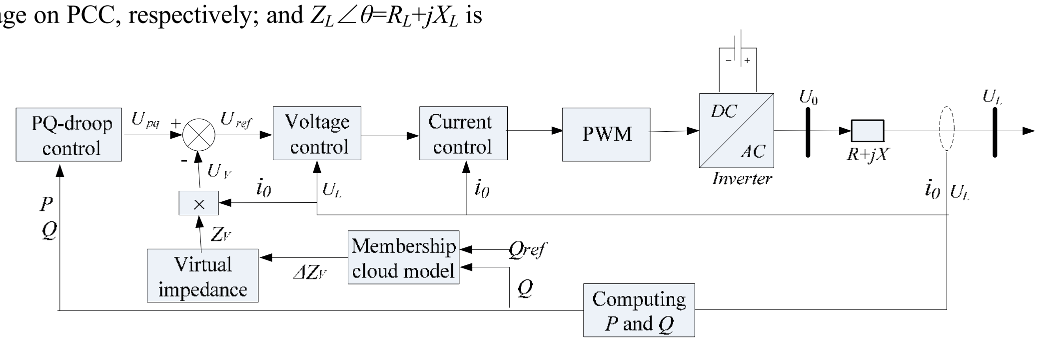

Fig. 2. Control strategy block on the cloud model theory to regulate ΔZ_V.

III. Droop Control with an Adjustable Virtual Impedance

A. Adjustable Virtual Impedance Concept

It is well known that not only imbalanced feeder impedances affect power sharing among the inverters, but also high R_L/X_L ratios deal with voltage raises. We set the virtual impedance as follows to overcome these disadvantages:

$$\vec{Z}_V = -R_L - \Delta R - j\omega\Delta X \tag{4}$$

Then the resistive part of the line becomes 0. The whole impedance of the line is:

$$\vec{Z}_T = j\omega X_L \tag{5}$$

In this case, the problems of *P/Q* couple and the imbalance line impedance can be solved. From the equations (1) and (2) it can be seen that after applying equation (4), the equations (1) and (2) can be expressed as:

$$\Delta U_T \approx \frac{X_L Q}{U_0} \tag{6}$$

$$\delta = \frac{X_L P}{U_0} \tag{7}$$

Equations (6) and (7) show that in the inductive impedance-dominated microgrids, the output *Q* controls the inverter voltage, while *P* controls the system frequency, independently. This behavior is similar that those in large power systems, so that similar equations can be found when transmitting power in large distances.

Then equation (4) can be rewritten as follows:

$$\vec{Z}_V = -R_L - \Delta Z_V \tag{8}$$

where $\Delta Z_V = \Delta R + j\omega\Delta X$ is the changing line impedance portion. In equation (8), although the value of R_L can be easily obtained, however the knowledge of the changing line impedance value is often not available. In this paper we propose a way to solve this problem by applying the cloud model theory to adjust ΔZ_V. The reactive power is inversely proportional to the line impedance. This relationship is used in the control method, which is shown in (6). The control diagram of the proposed approach is given in Fig. 2.

Fig. 2 shows the control strategy based on power/voltage/current three-loop including the proposed adjustable virtual impedance. As we know, communications among the parallel connected DGs can be reduced by the *P/Q* droop control method. The well-known traditional *P/Q* droop control functions can be expressed as:

$$\omega = \omega_0 - mP \tag{9}$$

$$U = U_0 - nQ \tag{10}$$

Where ω_0 and U_0 are the set frequency and voltage for micro-grid at no load conditions; m and n are the droop coefficients of DGs P and Q. Thus, the output voltage U_{pq} generated from the P/Q droop control can be shown as:

$$U_{pq} = U \sin \omega t \tag{11}$$

Thus, the reference for the voltage loop can be expressed as follows:

$$U_{ref} = U_{pq} - Z_V I \tag{12}$$

Where U_{ref} is the final reference voltage. In order to enhance Q-sharing accuracy, an adjustable virtual impedance strategy is proposed here. The cloud model theory is used to obtain the adjustable virtual impedance. We can implement the adjustable virtual impedance strategy straightly without the changing line impedance values.

B. the Cloud model Theory

We present the principle of the cloud model theory in this SubSection [10]. A membership cloud generator is constructed by three digital characteristics, which can cloud numerical values. Assuming that $R(E_x, H_e)$ is a random function, which meets a normal distribution. So the normal random entropy can be gotten:

$$E_n^{'} = R(E_n, H_e) \tag{13}$$

Where E_x is the expected value of a membership cloud. It shows the center of gravity of the cloud. E_n is the entropy to measure the fuzziness of the concept over the universe of discourse. H_e is the super-entropy to measure of the randomness of the membership function. Therefore, we can get the normal random number by the random function with an expected value E_x and the standard error $E_n^{'}$:

$$x_i = R(Ex, E_n^{'}) \tag{14}$$

The membership function with a normal distribution can be expressed as:

$$\mu_i = \exp\{\frac{-(x_i - Ex)^2}{2E_n^{'2}}\} \tag{15}$$

where x_i with membership μ_i is a cloud drop, which is drop(x_i , μ_i).

Hence, lots of cloud drops construct the membership cloud. Actually, we also call the membership cloud generator as the membership cloud generator with *X*-term.

Here, we say that it has a membership cloud generator with *Y*-term, if the set μ_i has a membership degree and it satisfies:

$$z_i = E_x \pm \sqrt{-2\ln(\mu_i)} E_n^{'} \tag{16}$$

A set of special cloud rules is established by using cloud generators with *X*-term and *Y*-term. These special cloud rules can be summed up by human controllers from their experiences. Note that the nonlinear characteristics can be expressed by these specified cloud rules . For example *"if A, then B"*, if the digital characteristics of the linguistic terms A and B in that rule are given. The membership degree, μ_i , produced by the cloud generator with *X*-term CG_X represents the activated strength of the rule which goes to control the cloud generator with *Y*-term CG_Y to produce a set of drops(z_i, μ_i) quantitatively. All the activated rules will make contributions to a particular input. This natural rule with one "and" can be constructed by the two-dimension membership cloud generator with *X*-term and the one-dimension membership cloud generator with *Y*-term, for example, "If A and B, then C" .

Set GA((E_{xx} E_{xy}),(E_{nx} E_{ny}),(H_{ex}, H_{ey})) be a two-dimension membership cloud, if there are

$$E_{nx}^{'} = R(E_{nx}, H_{ex}) \tag{17}$$

$$E_{ny}^{'} = R(E_{ny}, H_{ey}) \tag{18}$$

$$\mu(x,y) = \exp\{\frac{-(x - E_{xx})^2}{2E_{nx}^{'2}} + \frac{-(y - E_{xy})^2}{2E_{ny}^{'2}}\} \tag{19}$$

Thus we can get the two-dimension membership cloud generator with *X*-term.

According to equations (15) and (19), equation (19) can be represented as following:

$$\begin{aligned} \mu(x,y) &= \exp\{\ln(\mu(x)) + \ln(\mu(y))\} \\ &= \exp\{\ln(\mu(x)\mu(y))\} = \mu(x)\mu(y) \end{aligned} \tag{20}$$

Finally, the backward cloud generator is used to obtain the numerical output. The output expected value of E_{xu} expressed by:

$$E_{xu} = \frac{1}{n}\sum_{i=1}^{n} z_i \tag{21}$$

being numerical output expressed in (21). It is not necessary to calculate the output entropy E_{nu} and the output super-entropy H_{eu} here.

C. Adjusting the Virtual Impedance

The membership cloud model can convert the qualitative knowledge into the quantitative. The membership cloud model joins the fuzziness into randomness through E_x , E_n, and H_e for an object. The two-dimension and one-dimension membership cloud generator can form the control rules according to regulating actions. By using this method, the mathematical model is not necessary. It only requires controller's experience and their logic judgments to overcome the nonlinearities and uncertainties of the plant.

The Block diagram of the closed loop system using the cloud model theory to regulate the virtual impedance is shown in Fig. 3. In this control system, the error and the error change of the reactive power is settled as the input signal denoting as e and e_c, respectively. According to the input signals error e and the error change e_c, the variable term of the adjustable virtual impedance ΔZ_V can be obtained by applying the cloud model for online regulation purposes.

In Fig. 3, we set the input signals of the closed loop system t as e and e_c of reactive power Q. The output signal of the closed loop system is set as the changing virtual impedance ΔZ_V for the parameter regulation algorithm. There are three main steps in the computation process of the cloud model: (i) transforming input numerical values into clouds, (ii) setting reasoning rules and clouding uncertainty reasoning and (iii) transforming output clouds into numerical values.

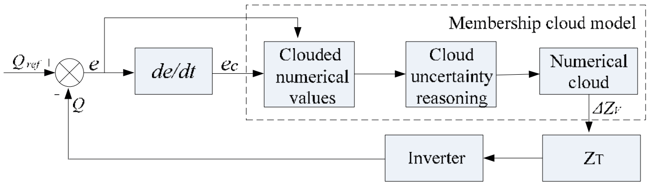

Fig. 3. Block diagram of the closed loop system to regulate the virtual impedance.

The discourse domains of input and output signals can be represented as [X_{min}, X_{max}]. So that the discourse domains of the error e and the error change e_c are [-1000 1000] and ΔZ_V [-1 1]. Here, in order to obtain three digital characteristics of each cloud, the golden section method is adopted[11]. The input and output signals e, e_c and ΔZ_V for the cloud model are expressed as Ge(E_x, E_n, H_e), Gec and GΔZ_V, respectively.

Subsequently, seven clouds of the error e can be expressed as:

E_{-3}=Ge1(-1000 333.3 42), E_{-2}= Ge2(-382 206.0 26),
E_{-1}= Ge3(-191 127.3 16), E_0= Ge4(0 78.7 10),
E_{+1}= Ge5(191 127.3 16), E_{+2}= Ge6(382 206.0 26),
E_{+3}=Ge7(1000 333.3 42).

Thus, the seven clouds of the error change e_c are:

EC_{-3}=Ge1(-1000 333.3 42), EC_{-2}= Ge2(-382 206.0 26),
EC_{-1}= Ge3(-191 127.3 16), EC_0= Ge4(0 78.7 10),
EC_{+1}= Ge5(191 127.3 16), EC_{+2}= Ge6(382 206.0 26),
EC_{+3}=Ge7(1000 333.3 42).

Hence the seven clouds of the changing virtual impedance ΔZ_V can be obtained by:

ΔZ_{V-3}=Ge1(-1 0.3 0.042), ΔZ_{V-2}= Ge2(-0.4 0.2 0.026),
ΔZ_{V-1}= Ge3(-0.2 0.1 0.016), ΔZ_{V0}= Ge4(0 0.08 0.01),
ΔZ_{V+1}= Ge5(0.2 0.1 0.016), ΔZ_{V+2}= Ge6(0.4 0.2 0.026),
ΔZ_{V+3}=Ge7(1 0.3 0.042).

The membership cloud of error e with 1000 cloud drops is shown in Fig.4. The membership cloud of the error changes e_c. We can get the membership cloud of the output ΔZ_V in the same way.

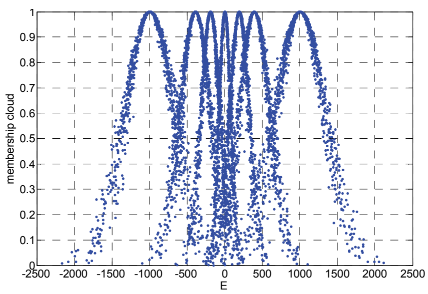

Fig. 4. Membership clouds of the error of the reactive power Q.

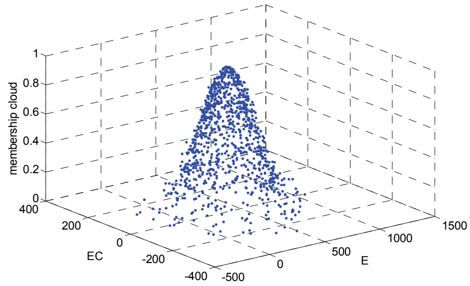

Fig. 5. Two-dimension membership cloud.

The two-dimension membership cloud is shown in Fig. 5 at "*if* E_{+2} *and* EC_0". Here the cloud drop number is also 1000. The two-dimension membership constructs each reasoning rule.

Cloud models of input and output signals e, e_c, and ΔZ_V, can be defined respectively According to corresponding each 7-cloud, as following:

E={NB,NM,NS,Z,PS,PM,PB}
EC={NB,NM,NS,Z,PS,PM,PB}
ΔZ_V ={NB,NM,NS,Z,PS,PM,PB}

being NB, NM, NS, Z, PS, PM, and PB, remark negative big, negative middle, negative small, zero, positive small, positive middle, and positive big, respectively. The reasoning rules for ΔZ_V are formed, which is given in Table I. For instance, if E is NB and EC is NB, then ΔZ_V is PB.

TABLE I. REASONING RULES OF ΔZ_V

E	EC						
	NB	NM	NS	Z	PS	PM	PB
NB	PB	PB	NB	PM	PS	PS	Z
NM	PB	PB	NM	PM	PS	Z	Z
NS	PM	PM	NS	PS	Z	NS	NM
Z	PM	PS	Z	Z	NS	NM	NM
PS	PS	PS	Z	NS	NS	NM	NM
PM	Z	Z	NS	NM	NM	NM	NB
PB	Z	NS	NS	NM	NM	NB	NB

In the process of the cloud reasoning shown in Fig. 6, CG_{Xi}, CG_{Yi} and CG_C are the two-dimension membership cloud generator with X-term, the one-dimension membership cloud generators with Y-term, and the backward membership cloud generator, respectively; 3E is a rule that cloud drops at the universe of discourse U, which is mainly contributing to the qualitative conception C to be in the range [E_x-3E_n, E_x+3E_n]. The 3E rule is given as follows. At the universe of discourse U, any $\triangle x$ at X which contributes to the qualitative conception C will guarantee the following approximation:

$$\Delta C \approx \frac{e^{-(x-E_x)^2/2E_n^2} \times \Delta x}{\sqrt{2\pi}E_n} \tag{22}$$

Obviously, there is:

$$\frac{\int_{E_x-3E_n}^{E_x-3E_n} e^{-(x-E_x)^2/2E_n^2} \times dx}{\sqrt{2\pi}E_n} = 99.74\% \qquad (23)$$

So that the quantified data contributed to the qualitative conception C is mainly inside the interval [E_x-3E_n, E_x+3E_n]. The other quantified data out of the region can be neglected.

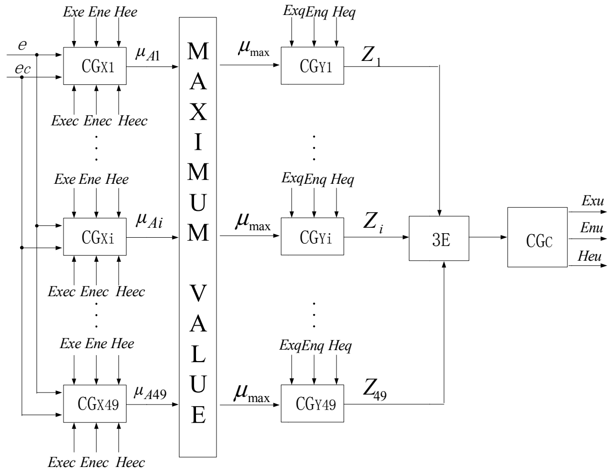

Fig. 6. Reasoning process to obtain the changing virtual impedance.

Input signals of the error e and the error change e_c are firstly transferred into natural linguistic terms, which activate the two-dimension cloud generator CG_{Xi} (i=1,2,⋯,n; here n=49). CG_{Xi} produces a group of random memberships μ_{Xi}=μ_{ij} (j=1,2,⋯, m) here m=1000. The group of memberships represents the activating strength for corresponding rule. One of rules with membership μ_{max} is selected, which is the input of CG_{Yi}. Then CG_{Yi} produces m drops Z_i with μ_{max} (i=1，2，⋯，m). If Z_i with μ_{max} satisfies the 3E rule, put Z_i belonging to [E_x-3E_n, E_x+3E_n] into CGc. Finally, the E_{xu} is the numerical output. The wanted ΔZ_V is actually the E_{xu}.

IV. Simulation and Analysis

A structure of the microgrid with two DGs is simulated to test the validation of the proposed control strategy in the Matlab. The DC voltage of each DG is 500V. The output voltage of each inverter is set peak value 311V with frequency 50Hz. The common load contains a resistor R_{Load}=10Ω and an inductor X_{Load} =1mH. Each DG is terminated by an LC filter with the following values: L=3mH and C=150μF. The feeder impedances are R_{L1}=0.5Ω and X_{L1}=1mH for DG1 and R_{L2}=0.8Ω and X_{L2}=2.5mH for DG2.

We compare the proposed droop control method with the conditional droop control method with the different line impedance. Figs. 7 and 8 are the corresponding simulating results.

The proposed control has good performance according to the simulating results shown in Fig. 7. The three-phase voltages at the PCC are shown in Fig.7(a). The voltage waveforms are sinusoidal. The difference between the ideal three-phase voltage and the real three-phase voltage waveforms at the PCC is given in Fig. 7(b). Note that only small voltage differences (about 5V) can be observed. Fig. 7(c) shows P and Q waveforms from DG1 and DG2. Notice the good P/Q sharing that can be obtained by using the proposed approach.

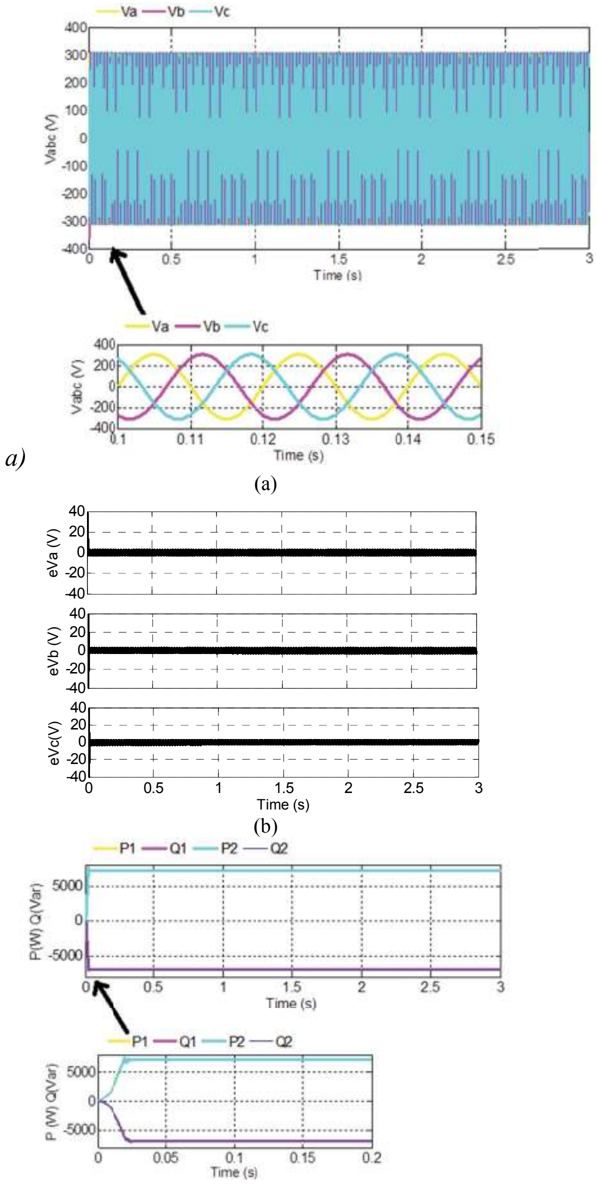

Fig. 7. Simulating results of the proposed control: (a) three-phase voltages at PCC, (b) the differences of three-phase voltages at PCC, (c) P and Q of DG1 and DG2.

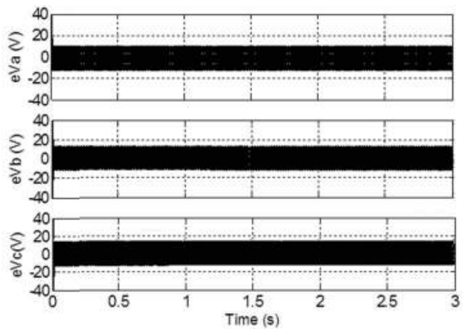

(a)

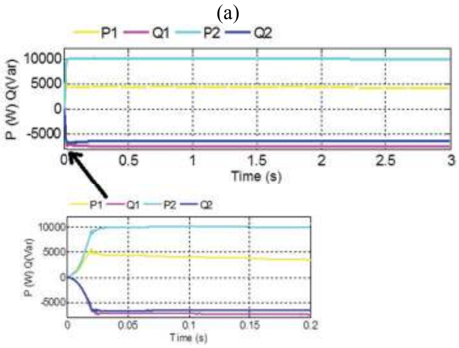

(b)

Fig. 8. Simulating results of the conventional droop control: (a) differences of three-phase voltages at PCC, (b) P and Q from DG1 and DG2.

The simulating results of the conventional droop control at the same conditions are shown in Fig.8. The three-phase voltage waveforms at PCC present a similar goodness, so they are not shown here. However, from the Fig.8(a) it can be seen that the differences between inverter voltages are bigger than these of the proposed control. As a conclusion, the performance of the proposed control method is better than that of the traditional droop control method. Note that by using this last one, *P/Q* cannot be properly shared due to the imbalanced feeder impedances.

From Fig.7 and 8, it can seen that the proposed control can track the changing line impedance values and achieve good power sharing thanks to the use of the proposed tunable virtual impedance loop. Notice that in this case both the three-phase voltages at PCC and the *P/Q* sharing are well performed.

V. Conclusion

A droop control equipped by an adjustable virtual impedance loop is proposed in this paper. The approach is based on the cloud model theory to adjust the changing virtual impedance in order to avoid *P/Q* coupling by compensating imbalanced line impedances. The cloud model can successfully bridge the gap between quantitative and qualitative methodologies when researching phenomenon uncertainties. Thus, the cloud model theory is applied well to adjust the virtual impedance loop with the changing line impedances according to the reactive power *Q* changes. The obtained simulating results points out the superiority of the proposed control method in front of the conventional droop method.

References

[1] M. C. Chandorkar, D. M. Divan, and R. Adapa, “Control of parallel connected inverters in standalone ac supply systems,” *IEEE Trans. Ind. Appl.*, vol. 29, no. 1, pp. 136–143, Jan.1993.

[2] J. Kim, J. M. Guerrero, P. Rodriguez, R. Teodorescu, and K. Nam, “Mode adaptive droop control with virtual output impedances for an inverter based flexible AC microgrid,” *IEEE Trans. Power Electron.*, vol. 26, no. 3, pp. 689–701, Mar.2011.

[3] Y. W. Li and C.-N. Kao, “An accurate power control strategy for power electronics-interfaced distributed generation units operating in a low voltage multibus microgrid,” *IEEE Trans. Power Electron.*, vol. 24, no. 12,pp. 2977–2988, Doc.2009.

[4] R. I. Bojoi, L. R. Limongi, D. Roiu, and A. Tenconi, “Enhanced power quality control strategy for single phase inverters in distributed generation systems,” *IEEE Trans. Power Electron.*, vol. 26, no. 3, pp. 798–806, Mar.2011.

[5] J. He, Y. W. Li, and S. Munir, “A flexible harmonic control approach through voltage controlled DG-grid interfacing converters,” *IEEE Trans. Ind. Electron.*, vol. 59, no. 1, pp. 444–455, Jan.2012.

[6] C. Wang, Z. Xiao, S. Wang, “Multiple feedback loop control scheme for inverters of the micro source in microgrids.” *Transactions of China Electrotechnical Society*, vol.24, no.2, pp.100-107, Feb.2009.

[7] J. M. Guerrero, J. C. Vasquez, J. Matas, et al. “Hierarchical control of droop-controlled AC and DC Microgrids-A general approach toward standardization,” *IEEE Transactions on Industrial Electronics*, vol.58, no.1, pp.158-172, Jan.2011.

[8] J. M. Guerrero, J. Matas, L. G. de Vicuna, M. Castilla, and J. Miret, “Decentralized control for parallel operation of distributed generation inverters using resistive impedance,” *IEEE Trans. Ind. Electron.*, vol. 54, no. 2, pp. 994–1004, Feb.2007.

[9] J. He, Y. W. Li, “Analysis, Design, and Implementation of Virtual Impedance for Power Electronics Interfaced Distributed Generation,” *IEEE Trans. Ind. App.*, vol. 47, no. 6, pp. 2525-2538, Jun.2011.

[10] D. Li, D. Cheung, X. Shi, “Uncertainty Reasoning Based on Cloud Models in Controllers”, *Computers Mathematic Application*, vol.35, no.3, pp. 99-123, Mar.1998.

[11] Y. Li, X. Fan, “Recursive integral proportional–integral control based on membership cloud for active power filter”, *IET Power Electron.,* Vol. 7, no. 11, pp. 2870–2876, Jul.2014.